AD-A043 902   AIRESEARCH MFG CO OF ARIZONA PHOENIX   F/G 20/4
AN EQUATION SPLITTING METHOD FOR SHOCK BOUNDARY LAYER INTERACTI--ETC(U)
JUL 77 P R DODGE, L S LIEBER   N00014-74-C-0317

UNCLASSIFIED   21-2548   NL

1 OF 1
AD
A043902

END
DATE
FILMED
9 -77
DDC

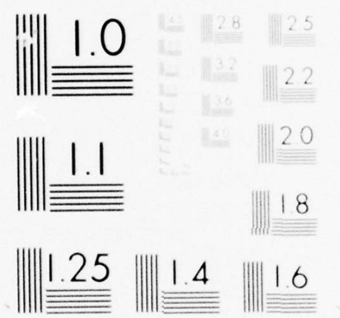

MICROCOPY RESOLUTION TEST CHART
NATIONAL BUREAU OF STANDARDS-1963-A

AD A043902

(12)
B.S.

AIRESEARCH REPORT 21-2548

AN EQUATION SPLITTING METHOD FOR SHOCK BOUNDARY LAYER INTERACTION

P. R. DODGE AND L. S. LIEBER
AIRESEARCH MANUFACTURING COMPANY OF ARIZONA
A DIVISION OF THE GARRETT CORPORATION
402 S. 36TH STREET, P. O. BOX 5217
PHOENIX, ARIZONA 85010

31 JULY 1977

Technical Report for Period 15 June 1974 - 31 May 1977

Approved for public release; distribution unlimited.

Prepared for

DEPARTMENT OF THE NAVY
OFFICE OF NAVAL RESEARCH
ARLINGTON, VIRGINIA 22217
Under Contract No. N00014-74-C-0317
Task No. NR 061-221

NOTICE

When Government drawings, specifications, or other data are used for any purpose other than in connection with a definitely related Government procurement operation, the United States Government thereby incurs no responsibility nor any obligation whatsoever; and the fact that the government may have formulated, furnished, or in any way supplied the said drawings, specifications, or other data, is not to be regarded by implication or otherwise as in any manner licensing the holder or any other person or corporation, or conveying any rights or permission to manufacture, use, or sell any patented invention that may in any way be related thereto.

UNCLASSIFIED

SECURITY CLASSIFICATION OF THIS PAGE (When Data Entered)

REPORT DOCUMENTATION PAGE		READ INSTRUCTIONS BEFORE COMPLETING FORM
1. REPORT NUMBER AiResearch Report 21-2548	2. GOVT ACCESSION NO.	3. RECIPIENT'S CATALOG NUMBER
4. TITLE (and Subtitle) (6) AN EQUATION SPLITTING METHOD FOR SHOCK BOUNDARY LAYER INTERACTION		5. TYPE OF REPORT & PERIOD COVERED Final Report
(14)		6. PERFORMING ORG. REPORT NUMBER 21-2548
7. AUTHOR(s) (10) P. R. Dodge L. S. Lieber	(15)	8. CONTRACT OR GRANT NUMBER(s) N00014-74-C-0317
9. PERFORMING ORGANIZATION NAME AND ADDRESS Garrett Corporation AiResearch Manufacturing Co. of Arizona Phoenix, Arizona 85034		10. PROGRAM ELEMENT, PROJECT, TASK AREA & WORK UNIT NUMBERS NR 061-221
11. CONTROLLING OFFICE NAME AND ADDRESS Department of the Navy Office of Naval Research Arlington, Virginia 22217	(11)	12. REPORT DATE 31 July 1977
		13. NUMBER OF PAGES 48
14. MONITORING AGENCY NAME & ADDRESS(if different from Controlling Office) (12) 39p.		15. SECURITY CLASS. (of this report) Unclassified
		15a. DECLASSIFICATION/DOWNGRADING SCHEDULE

16. DISTRIBUTION STATEMENT (of this Report)

Approved for public release; distribution unlimited

17. DISTRIBUTION STATEMENT (of the abstract entered in Block 20, if different from Report)

(9) Final rept. 15 Jun 74-31 May 77,

18. SUPPLEMENTARY NOTES

19. KEY WORDS (Continue on reverse side if necessary and identify by block number)

Separated Flow
Shock Boundary Layer
Equation Splitting Method

20. ABSTRACT (Continue on reverse side if necessary and identify by block number)

An equation splitting numerical method for compressible separated flow is described. The basic equations are developed and solved. Comparison to a laminar shock boundary layer interaction is made. Results show qualitative agreement with discrepancies attributed to detail inaccuracies in the numerical methods. Rapid convergence and low computation times are realized.

DD FORM 1 JAN 73 1473 EDITION OF 1 NOV 65 IS OBSOLETE

UNCLASSIFIED

SECURITY CLASSIFICATION OF THIS PAGE (When Data Entered)

404 796

mt

UNCLASSIFIED

SECURITY CLASSIFICATION OF THIS PAGE(When Data Entered)

UNCLASSIFIED

SECURITY CLASSIFICATION OF THIS PAGE(When Data Entered)

PREFACE

AiResearch Manufacturing Company of Arizona has conducted a research study for the Office of Naval Research under Contract N00014-74-C-0317, Task NR 061-221, to develop rapid efficient techniques for Navier-Stokes solutions. This document reports the last year's activity. Previous activities have been reported and are referenced herein.

TABLE OF CONTENTS

LIST OF ILLUSTRATIONS

SECTION I
INTRODUCTION

Traditional techniques of solving the Navier-Stokes equations for compressible separated flow have utilized time-dependent methods. These methods have, with extensive development, steadily improved in both accuracy and computational times. Recently, however, Dodge[1] and Dodge and Lieber[2] have introduced a new steady-state solution method for incompressible flow that splits the pressure and shear forces into two separate equations. One equation is elliptic, and the other nearly parabolic. Contained herein is a description of the first attempt to extend this method to compressible flow. Application is made to the interaction of an oblique shock wave with a laminar boundary layer. The development was guided by the realization that the ultimate value of such a method lies not in the solution of two-dimensional laminar shock boundary layer interactions, but rather in applications to more complete two-dimensional and three-dimensional geometries. Although more development to improve accuracy and further reduce computational times is suggested, the results to date demonstrate the general viability of this numerical method. The following sections describe in detail the basic equation development, numerical techniques, results of the calculations, and suggestions for accuracy improvements.

SECTION II
EQUATION DEVELOPMENT

The basis of Dodge's equation-splitting solution method lies in the separation of equations describing pressure and viscous effects. To accomplish this separation, the velocity vector $\vec{W}$ is expressed in the following manner:

$$\vec{W} = \nabla\phi + \vec{U} \tag{1}$$

where ϕ = velocity potential

$\vec{U}$ = velocity vector reflecting viscous effects (viscous loss velocity vector)

Equations are then required to solve individually for ϕ and $\vec{U}$.

As an initial step, consider the vector form of the momentum equation for steady laminar flow:

$$\rho(\vec{W}\cdot\nabla)\vec{W} = -\nabla P + \nabla(\lambda\nabla\cdot\vec{W}) + \nabla\cdot(\mu\,\mathrm{def}\vec{W}) \tag{2}$$

where ρ = density

P = static pressure

μ = molecular viscosity

λ = second coefficient of viscosity

$$\mathrm{def}\vec{W} = \nabla\vec{W} + (\nabla\vec{W})^*$$

$$(\nabla\vec{W})^* = \text{transpose } (\nabla\vec{W})$$

Equation (1) may then be substituted for $\vec{W}$ in Equation (2) as follows:

$$\begin{aligned} &\rho\ \nabla\phi\cdot\nabla(\nabla\phi) + \rho\vec{U}\cdot\nabla(\nabla\phi) + \rho(\vec{W}\cdot\nabla)\vec{U} \\ &\quad = -\nabla P + \nabla(\lambda\nabla\cdot\vec{W}) + \nabla\cdot(\mu\mathrm{def}\vec{W}) \end{aligned} \tag{3}$$

To treat the static pressure gradient in Equation (3), consider the density to be described by two terms -- one, ρ^*, related to static pressure and the other, ρ_v, related to viscous effects:

$$\rho = \rho^* + \rho_v \tag{4}$$

The density component ρ^* is defined by

$$\rho^* = \rho_I'\left(1 - \frac{\nabla\phi\cdot\nabla\phi}{2C_pT_I'}\right)^{\frac{1}{\gamma-1}} \tag{5}$$

where

ρ_I' = reference condition of stagnation density

T_I' = reference condition of stagnation temperature

C_p = specific heat at constant pressure

γ = ratio of specific heats

Further, one can show that all possible static pressure gradients may be represented by

$$- \nabla P = \rho^{*} \nabla\phi \cdot \nabla(\nabla\phi) \tag{6}$$

where ρ^{*} is selected so that the right-hand side of Equation (6) is irrotational. Substituting Equation (4) into Equation (3), combining terms, and using Equation (6) yields

$$\begin{aligned}(\rho - \rho^{*})\nabla\phi\cdot\nabla(\nabla\phi) + \rho\vec{U}\cdot\nabla(\nabla\phi) + \rho(\vec{W}\cdot\nabla)\vec{U} \\ = \nabla(\lambda\nabla\cdot\vec{W}) + \nabla\cdot(\mu \mathrm{def}\vec{W})\end{aligned} \tag{7}$$

Equations (6) and (7) could then provide the basis for separate equations for ϕ and $\vec{U}$, respectively. However, when Equation (6) is combined with the continuity equation and the equation of state, it yields a relation that becomes hyperbolic for supersonic conditions based upon potential rather than total velocity. To reconcile this difficulty, a different approach was taken in the development of the potential equation.

The pressure gradient may be expressed in terms of the equation of state, as

$$\nabla P = a^2\nabla\rho + a^2\rho\left(\frac{\gamma-1}{\gamma R}\right)\nabla S \tag{8}$$

where

a = local speed of sound at static conditions

R = gas constant

S = entropy

Replacing the pressure gradient term in the momentum equation, Equation (2), with Equation (8), and dotting the resulting expression with $\vec{W}$, yields Equation (9).

$$\begin{aligned}\vec{W}\cdot[\rho(\vec{W}\cdot\nabla)\vec{W}] = - a^2(\vec{W}\cdot\nabla\rho) - a^2\rho\left(\frac{\gamma - 1}{\gamma R}\right)\vec{W}\cdot\nabla S \\ + \vec{W}\cdot\nabla(\lambda\nabla\cdot\vec{W}) + \vec{W}\cdot[\nabla\cdot(\mu \mathrm{def}\vec{W})]\end{aligned} \tag{9}$$

The vector form of the compressible continuity equation, given by

$$\nabla\cdot(\rho\vec{W}) = 0 \tag{10}$$

may be expanded and re-expressed as

$$\vec{W}\cdot\nabla\rho = -\rho\nabla\cdot\vec{W} \qquad (11)$$

Substituting Equation (11) into the first term of the right-hand side of Equation (9), rearranging, and dividing by ρ, yields Equation (12).

$$\vec{W}\cdot[(\vec{W}\cdot\nabla)\vec{W}] - a^2(\nabla\cdot\vec{W}) = -a^2\left(\frac{\gamma - 1}{\gamma R}\right)\vec{W}\cdot\nabla S + \vec{W}\cdot\left[\frac{1}{\rho}\nabla(\lambda\nabla\cdot\vec{W})\right] + \vec{W}\cdot\left[\frac{1}{\rho}\nabla\cdot(\mu\,\mathrm{def}\vec{W})\right] \qquad (12)$$

However, Equation (12) may be recast by replacing $\vec{W}$ in the left-hand terms of Equation (12) with the velocity components of Equation (1). Then, placing all terms involving potential on the left-hand side of the resulting equation, and expanding the last two terms, yields the following:

$$\begin{aligned}\vec{W}\cdot[(\vec{W}\cdot\nabla)\nabla\phi] - a^2\nabla^2\phi &= a^2\nabla\cdot\vec{U} - \vec{W}\cdot[(\vec{W}\cdot\nabla)\vec{U}] \\ &- a^2\left(\frac{\gamma - 1}{\gamma R}\right)\vec{W}\cdot\nabla S + \vec{W}\cdot\left[\frac{1}{\rho}\nabla(\lambda\nabla\cdot\vec{W})\right] \qquad (13) \\ &+ \vec{W}\cdot\left\{\frac{\mu}{\rho}[\nabla(\nabla\cdot\vec{W}) + \nabla^2\vec{W}] + (\mathrm{def}\vec{W})\frac{\nabla\mu}{\rho}\right\}\end{aligned}$$

Equation (13) thus describes pressure effects in terms of the velocity potential, ϕ. The equation will be elliptic or hyperbolic, depending upon the local Mach number, defined in terms of the velocity, W.

The equation for the viscous loss velocity vector is developed from the momentum equation, as presented in Equation (7). The terms on the right-hand side of Equation (7) may be expanded in the same manner as for the incompressible case presented by Dodge[1]. Then, rearranging, and dividing the resulting equation by ρ, yields

$$\begin{aligned}\vec{U}\cdot\nabla(\nabla\phi) + (\vec{W}\cdot\nabla)\vec{U} &= \left(\frac{\rho^*}{\rho} - 1\right)\nabla\phi\cdot\nabla(\nabla\phi) \\ &+ \frac{1}{\rho}\{(\nabla^2\phi)\nabla\lambda + (\nabla\cdot\vec{U})\nabla\lambda + (2\mu + \lambda)\nabla(\nabla^2\phi) \\ &+ (\mu + \lambda)\nabla(\nabla\cdot\vec{U}) + \mu\nabla^2\vec{U} + 2[\nabla(\nabla\phi)]^*\nabla\mu \\ &+ (\mathrm{def}\vec{U})\nabla\mu\} \qquad (14)\end{aligned}$$

When expanded, Equation (14) will produce scalar equations for the viscous loss velocity components, U_i. These equations may be parabolized by treating the streamwise diffusion term as a known quantity from the previous iteration, as discussed by Dodge[1] and Dodge and Lieber[2].

Because the flow is compressible, an energy equation is also required. In terms of static enthalpy, the laminar steady-flow energy equation may be given as

$$\rho(\vec{W}\cdot\nabla)(h + \frac{1}{2}W^2) = \nabla\cdot(\lambda\vec{W}\nabla\cdot\vec{W}) + \nabla\cdot(\vec{W}\cdot\mu\mathrm{def}\vec{W}) + \nabla\cdot(k\nabla T) \qquad (15)$$

where

h = enthalpy at static conditions

k = conductivity of the fluid

T = static temperature

Expressing enthalpy in terms of static temperature, i.e.,

$$h = C_p T \qquad (16)$$

and expanding the left-hand side of Equation (15), yields Equation (17)

$$\rho(\vec{W}\cdot\nabla)(C_pT) + \frac{1}{2}\rho(\vec{W}\cdot\nabla)W^2 = \nabla\cdot(\lambda\vec{W}\nabla\cdot\vec{W}) + \nabla\cdot(\vec{W}\cdot\mu\mathrm{def}\vec{W}) + \nabla\cdot(k\nabla T) \qquad (17)$$

Assuming a constant Prandtl number, Pr, given by

$$Pr = \frac{\mu C_p}{k} \qquad (18)$$

then conductivity may be expressed as

$$k = \frac{\mu C_p}{Pr} \qquad (19)$$

In addition, specific heat is assumed to be constant. Thus, substituting Equation (19) into Equation (17), rearranging, and dividing by ρC_p, yields

$$(\vec{W}\cdot\nabla)T - \frac{1}{\rho C_p}\nabla\cdot[(\frac{\mu C_p}{Pr})\nabla T]$$
$$= \frac{1}{\rho C_p}[-\frac{1}{2}\rho\ (\vec{W}\cdot\nabla)W^2 \tag{20}$$
$$+ \nabla\cdot(\lambda\vec{W}\nabla\cdot\vec{W}) + \nabla\cdot(\vec{W}\cdot\mu\text{def}\vec{W})]$$

Expanding the second term on the left-hand side of Equation (20) results in the following:

$$(\vec{W}\cdot\nabla)T - \frac{1}{\rho Pr}[\nabla\mu\cdot\nabla T + \mu\nabla^2 T]$$
$$= \frac{1}{\rho C_p}[-\frac{\rho}{2}(\vec{W}\cdot\nabla)W^2 + \nabla\cdot(\lambda\vec{W}\nabla\cdot\vec{W})$$
$$+ \nabla\cdot(\vec{W}\cdot\mu\text{def}\vec{W})] \tag{21}$$

Expanding the last two terms of Equation (21) yields

$$(\vec{W}\cdot\nabla)T - \frac{1}{\rho Pr}(\nabla\mu\cdot\nabla T) - \frac{1}{\rho Pr}(\mu\nabla^2 T)$$
$$= \frac{1}{\rho C_p}\{-\frac{\rho}{2}(\vec{W}\cdot\nabla)W^2 + \lambda(\nabla\cdot\vec{W})^2$$
$$+ \mu\ [\nabla\cdot(\vec{W}\cdot\text{def}\vec{W}) - \vec{W}\cdot(\nabla\cdot\text{def}\vec{W})]$$
$$+ \vec{W}\cdot[\nabla(\lambda\nabla\cdot\vec{W}) + \nabla\cdot(\mu\text{def}\vec{W})]\} \tag{22}$$

Substituting the momentum equation in the form of Equation (7) for the last two terms in Equation (22) gives the final form of the laminar, steady-flow energy equation in terms of static temperature:

$$(\vec{W}\cdot\nabla)T - \frac{1}{\rho Pr}(\nabla\mu\cdot\nabla T) - \frac{1}{\rho Pr}(\mu\nabla^2 T)$$
$$= \frac{1}{\rho C_p}\{-\frac{\rho}{2}(\vec{W}\cdot\nabla)W^2 + \lambda\ (\nabla\cdot\vec{W})^2$$
$$+ \mu\ [\nabla\cdot(\vec{W}\cdot\text{def}\vec{W}) - \vec{W}\cdot(\nabla\cdot\text{def}\vec{W})]$$
$$+ \rho\vec{W}\cdot\ [\vec{U}\cdot\nabla(\nabla\phi) + (\vec{W}\cdot\nabla)\vec{U}$$
$$+ (1 - \frac{\rho^*}{\rho})\nabla\phi\cdot\nabla(\nabla\phi)]\} \tag{23}$$

As with the equation for $\vec{U}$, Equation (23) may be parabolized by treating the diffusion term as a known quantity from the previous iteration.

Equations (13), (14), and (23) comprise the system of equations that must be solved to yield ϕ, $\vec{U}$, and T. In conjunction with these equations, a set of boundary conditions is required. Figures 1 and 2 illustrate the boundary conditions on the solution space for the elliptic/hyperbolic and parabolic equations.

In Figure 1, the potential velocities V_I, V_M, and V_E are determined, based upon the oblique shock equations. The value of ϕ_E is determined by integrating the values of $\partial\phi/\partial x_1$ to the downstream boundary.

The upstream values of $\vec{U}$ and T in Figure 2 are dependent upon the corresponding value of $\vec{W}$, which is initialized using an arbitrary boundary layer profile similar to a Pohlhausen profile. An isothermal plate is assumed, with plate temperature equal to the reference stagnation temperature.

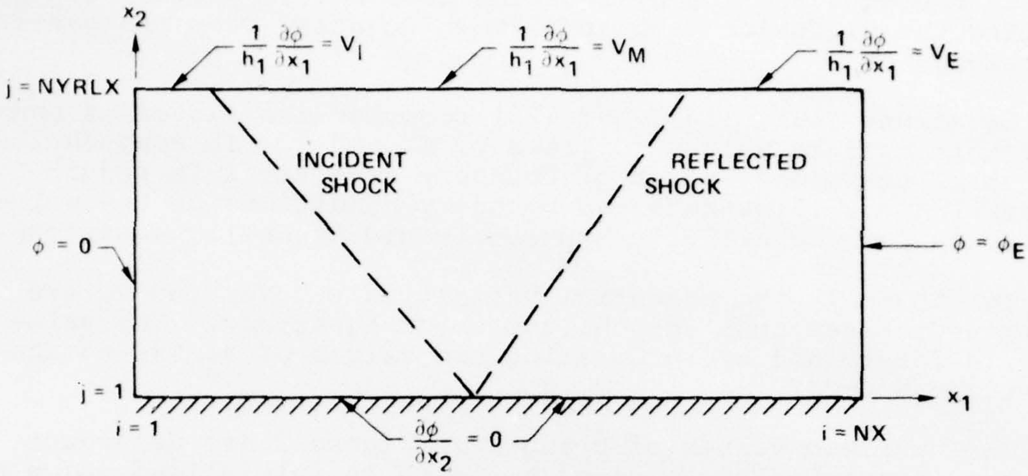

Figure 1. Boundary conditions on ϕ for elliptic/hyperbolic equation.

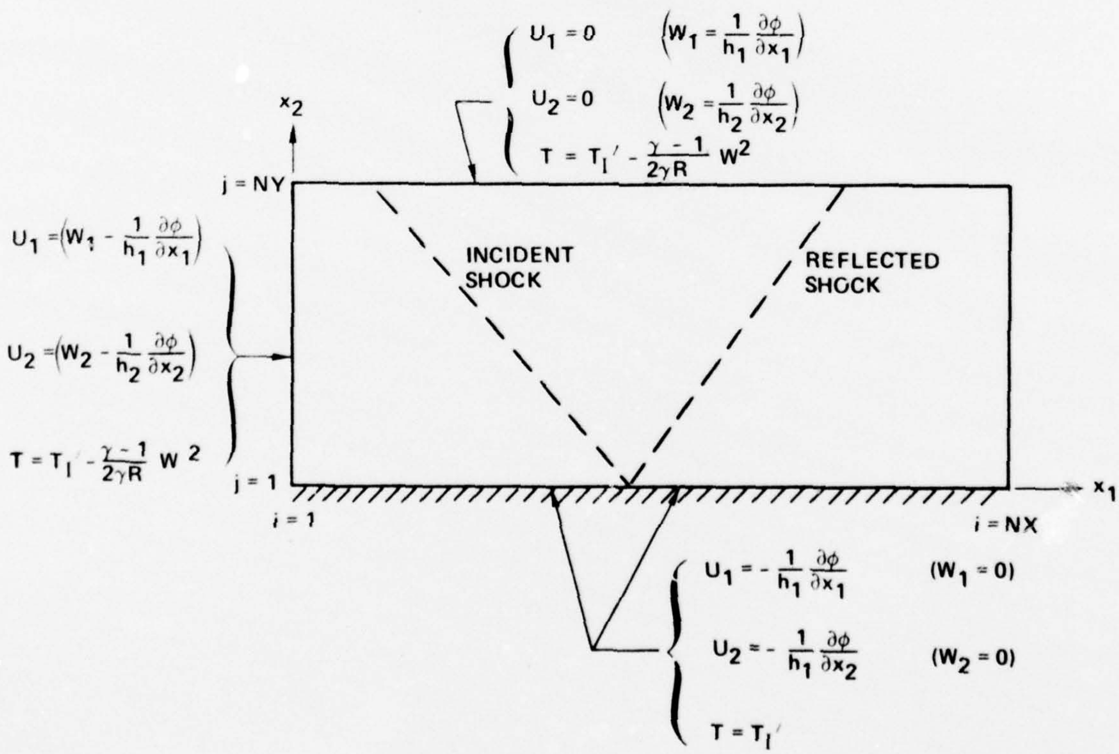

Figure 2. Boundary conditions on U_1, U_2, T for parabolic equation.

SECTION III
NUMERICAL METHODS

Two major numerical solutions are required to implement the above algorithm: a solution to a mixed elliptic/hyperbolic potential equation, and a solution to a nearly parabolic viscous-shear equation. Murman and Cole[3], in a pioneering paper, developed a technique for modifying a difference star with Mach number, and then using conventional relaxation to solve a similar equation. Modifications to the Murman and Cole method have been necessary to improve its accuracy, and allow its use in totally supersonic flow. Dodge[4,5] describes such a method and its application to supersonic inlet, subsonic exit compressor blades. Murman[6], in a subsequent paper, reported further improvements in the basic methods to account for differencing across discontinuities. From these works, a list of ideal characteristics can be assembled for the supersonic portion of any such algorithm.

- o Region of influence of difference star matches precisely the region of influence of the differential equation.
- o Across a potential slope discontinuity, the method must preserve the proper jump conditions.
- o The method remains integrally conservative in the non-discontinuous portion of the flow field.

Unfortunately, such a numerical method does not now exist.

To assist in the evaluation of the importance of each of the above criteria, the one-dimensional potential Equation (24) was studied.

$$(V^2 - a^2)\frac{d^2\phi}{dx^2} = 0 \qquad (24)$$

where

a = sound speed

$V = \frac{d\phi}{dx}$

ϕ = velocity potential

For the solution to be other than trivial, the flow must enter supersonically, undergo a jump, and exit subsonically. Boundary conditions then consist of an inlet Mach number and an exit potential. By integrating Equation (24) and assuming an ideal gas, a jump condition can be derived that relates downstream velocity to inlet velocity.

$$V_1 \left(a'^2 - \frac{\gamma + 1}{6} V_1^2\right)$$
$$= V_2 \left(a'^2 - \frac{\gamma + 1}{6} V_2^2\right) \qquad (25)$$

where

a' = stagnation speed of sound
γ = ratio of specific heats
V_1 = velocity ahead of the jump
V_2 = velocity behind the jump

The analytical solution ahead of and behind the jump is obviously that of constant velocity. Jump location is determined by matching to the exit potential boundary condition using Equation (26).

$$x_J = \frac{\phi_{EXIT} - V_2 L}{V_1 - V_2} \qquad (26)$$

where

x_J = position of the jump
L = total length of the solution region ($X = 0$ is the inlet)
ϕ_{EXIT} = exit potential

Consider what happens when the original Murman and Cole method is applied. Upstream of the assumed jump location, the difference star is cast in a backwards direction.

$$(\phi_i - 2\phi_{i-1} + \phi_{i-2}) = 0 \qquad (27)$$

where

ϕ_i = potential at the ith node

Note that the value of $V^2 - a^2$ is immaterial since it is a non-zero constant at any particular node, and thus divides out. Downstream of the assumed jump location, the equation is elliptic.

$$\phi_{i+1} - 2\phi_i + \phi_{i-1} = 0 \tag{28}$$

The solution to both Equations (27) and (28) is a linear variation in ϕ. An initial guess for potential would be made. Equation (27) is solved starting at node 3, and simply broadcasts forward the initial velocity gradient until a node is reached, which was initially assumed subsonic. At this point, the subsonic solution proceeds as a boundary value problem with ϕ at the change-over (supersonic to subsonic) point established by Equation (27). There is, however, no communication between upstream and downstream. Thus, the location of the jump never changes, and the value of the velocity at the jump is only controlled by the initial guess of jump location and potential variation. No aspect of the physical problem appears in the numerical solution at the jump. To overcome this, special conditions at the jump must be invoked, as pointed out by Murman[6]. It is, however, immaterial what form is used away from the jump. A conservative form results in a solution that is no different from a nonconservative form.

When actually applying methods to introduce upstream-downstream communication, two classes result. The first class, into which Murman's method falls, allows the downstream flow to be adjusted based on upstream conditions. This class allows only for jump propagation in the forward direction. The second class, permits the jump to retreat by allowing the upstream flow to be affected by downstream conditions. Whether the jump needs to retreat or go forward is only dependent on the initial guess, and thus, for complete generality, both classes must be combined into a single method. For one-dimensional flow, such techniques are readily generated, the results of which are shown in Figure 3 for a forward propagating jump and Figure 4 for a retreating jump. The jump-node region is treated by the following algorithm

$$D = r\phi_{i+1} + \phi_{i-1} - (1+r)\ \phi_i = 0$$

applied to the node ahead of the jump if $D \geq 0$,

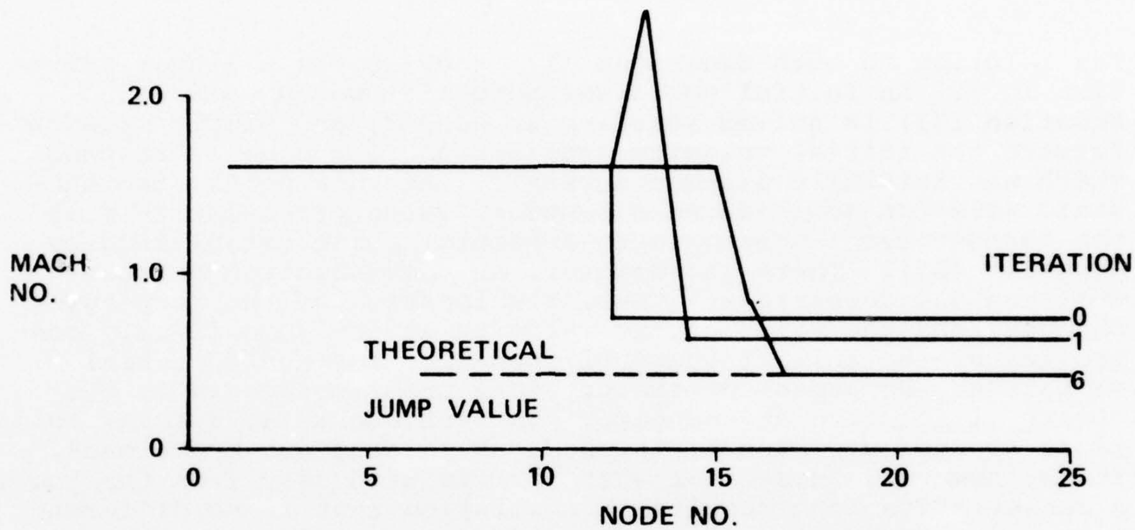

Figure 3. Forward propagating one-dimensional jump.

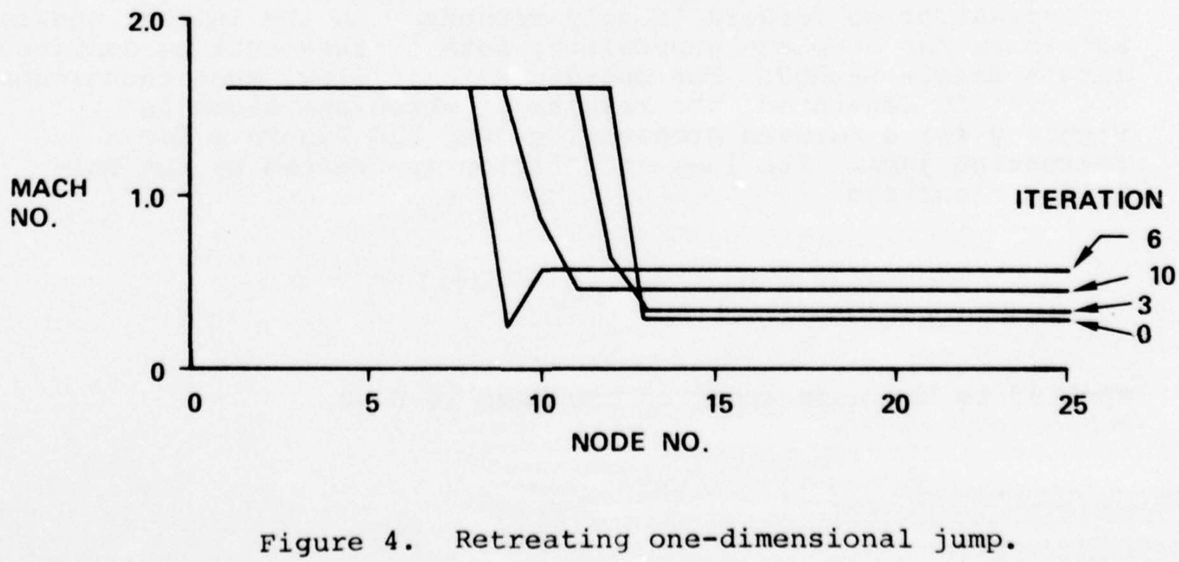

Figure 4. Retreating one-dimensional jump.

applied to the node behind the jump if D <0

$$r = \frac{\alpha_{DOWN}}{\alpha_{UP}}$$

$$\alpha = V(a'^2 - \frac{\gamma+1}{6} V^2)$$

where DOWN and UP subscripts refer to downstream and upstream of the jump.

It is necessary to evaluate the velocity away from the jump, since values at the jump, particularly for intermediate iterations, are in significant error.

When the flow field is multidimensional and jumps are other than normal, the proper procedure is complicated by the lack of accepted numerical solutions. Murman's method assumes an oblique jump passing through the grid system at an arbitrary angle. However, this derivation looses sight of the fact that the differential equation is left behind when solutions are made to the finite-difference grid. Discontinuities on a fixed orthogonal finite-difference system can only have one of three forms, illustrated by Figure 5. A physically oblique wave must be made up of discrete components of the three jumps. The normal jump causes little or no problems, but the other two result in differencing across a discontinuity. To be totally correct, as Murman points out, any difference scheme applied to any combination of the above discontinuities must be integrally (summation in difference system) conservative of the desired jump condition. Even if such a system existed, however, practical problems, such as detecting a jump and determining proper upstream and downstream conditions away from the perturbed region of the jump, intervene to prevent reliable treatment of jump conditions.

The method by Dodge[4] avoids some of the difficulty by only differencing along characteristic lines, and not differencing across oblique jumps, which may explain some of its good results. However, it requires a nonstationary grid system that is difficult to implement in two dimensions, and is nearly impossible in three dimensions. Thus, after comparing other methods, such as the two by Murman, to a range of six supersonic and supercritical cases, it was decided to mix a nonorthogonal and orthogonal difference system, staying with a fixed orthogonal grid system.

Figure 5. Possible jump nodes.

The degree of mixing was determined as a function of local Mach number, based upon a criterion developed from a stability analysis of the basic relaxation difference equation. Figure 6 illustrates the difference stars utilized. In simplified form, the mixing of difference operators is accomplished in the following following manner:

$$C_1 \frac{\partial^2\phi}{\partial x^2} + C_2 \frac{\partial^2\phi}{\partial y^2} = [C_1 \frac{\partial^2\phi}{\partial x^2} + C_2 \frac{\partial^2\phi}{\partial y^2}](f_H)$$

$$+ [C_1 \frac{\partial^2\phi}{\partial x^2} + C_2 \frac{\partial^2\phi}{\partial y^2}](1 - f_H)$$

where f_H represents the fraction of hyperbolic difference operator utilized, and $(1-f_H)$ represents the fraction of single-spaced implicit difference operator. The local value of f_H was determined for supersonic flow to be

$$f_H = -C_2/C_1 \text{ for } (-C_2/C_1) < 1.0$$

or

$$f_H = 1.0 \text{ for } (-C_2/C_1) \geq 1.0$$

based upon a stability analysis.

If the variable supersonic difference star is examined in relation to the location of local characteristic lines, it may be seen that, as Mach number increases, the difference star becomes weighted to more closely reflect the region of influence of the characteristic lines (refer to Figure 7), eventually becoming totally hyperbolic.

Admittedly, such a system does not meet all the criteria for a potential equation solver set out above, but represents a workable compromise between complete agreement with the above criterion, and the practical constraints of computer code development.

The viscous equation, on the other hand, represents a much easier form to implement. Dodge[1] and Dodge and Lieber[2] have discussed many of the difficulties associated with marching equation solution. For this program, the streamwise diffusion term was determined from the previous iteration. In separated flow regions, the difference star for the convection term was turned upstream, utilizing the values established on a previous iteration. With these adjustments, the solution to the viscous equation proceeds as a normal marching solution to a parabolic equation. The component of velocity normal to the wall in the

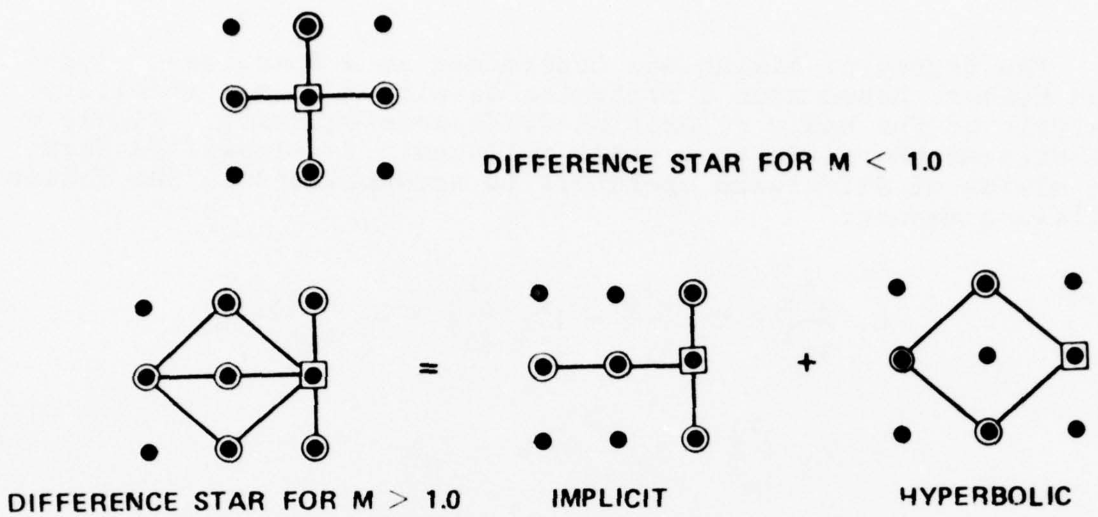

Figure 6. Transonic difference stars.

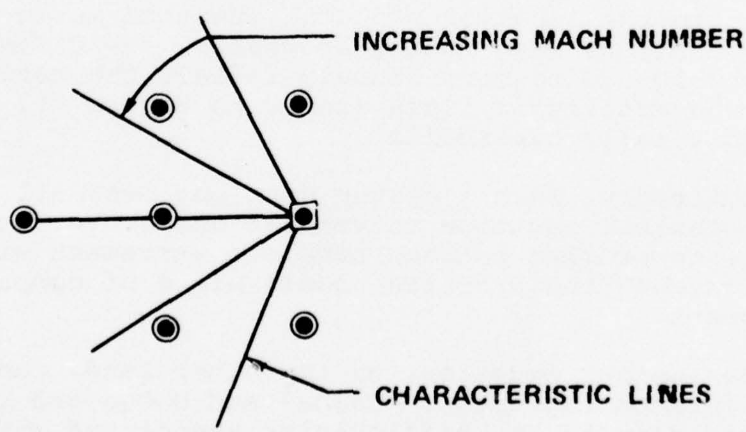

Figure 7. Supersonic difference star.

region between the wall node and the first relaxation node was, however, determined from the continuity equation. This was found in past studies by Dodge[1] to produce somewhat more accurate results.

The program developed to implement this numerical solution method consisted of a modularized code written in a structured FORTRAN language. A basic logic diagram for the program may be found in Figure 8.

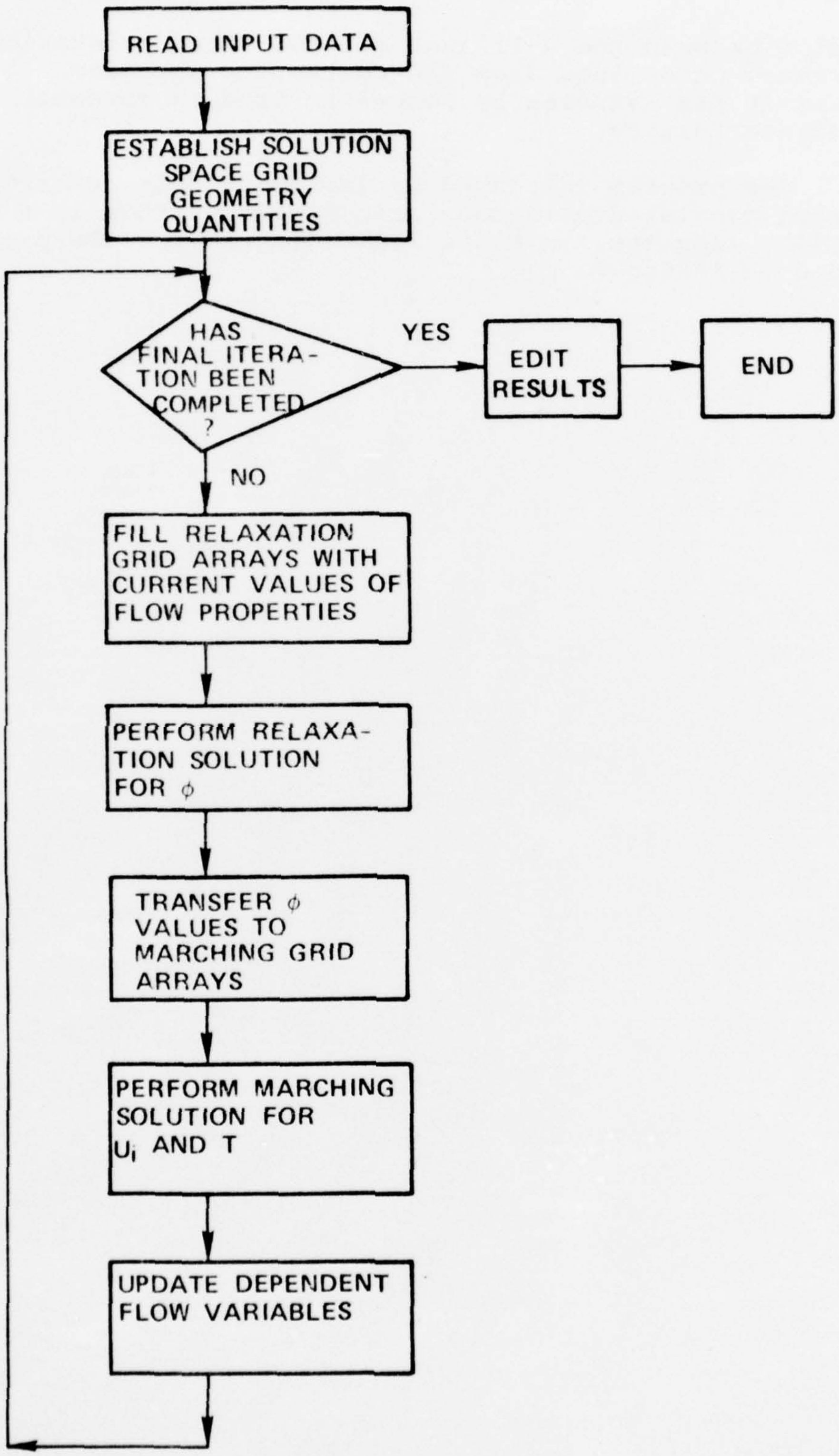

Figure 8. Program logic diagram.

SECTION IV
CALCULATION RESULTS

The numerical method discussed herein has been utilized to predict separation of a two-dimensional laminar flat-plate shock boundary layer interaction flow. The test case used was that of Hakkinen, et al[7], consisting of a laminar flat-plate flow with an upstream Mach number $M_o = 2.0$, and a Reynolds number $Re_L = 2.96 \times 10^5$, where

$$Re_L = \frac{W_o L}{\nu_o}$$

and

W_o = freestream inlet velocity (W_o = 1664 ft/sec)

ν_o = freestream inlet value of kinematic viscosity at static conditions

L = distance from leading edge to shock intersection with plate (L = 0.1624 ft)

An oblique shock wave, with shock angle $\theta = 32.59°$, intersects the flat plate as indicated in Figure 9.

The grid system employed in the numerical solution consisted of a linear relaxation grid and a marching grid composed of the relaxation nodes, with an additional nonlinear grid segment near the wall. This scheme permits a coarse grid to be used for the relaxation solution, and yet provides a more finely-spaced grid within the boundary layer for the viscous marching equation solution. Figure 10 illustrates the relative spacing of the relaxation and marching grid nodes within the boundary layer.

Results of the present numerical method were compared with both the experimental data of Hakkinen, and results of the time-dependent scheme of MacCormack[8].

Figure 11 compares surface pressure distribution for the three sets of data. Clearly, the pressure plateau in the region of the shock/plate intersection is not indicated by the present method. A much sharper pressure rise is predicted than evidenced by experiment.

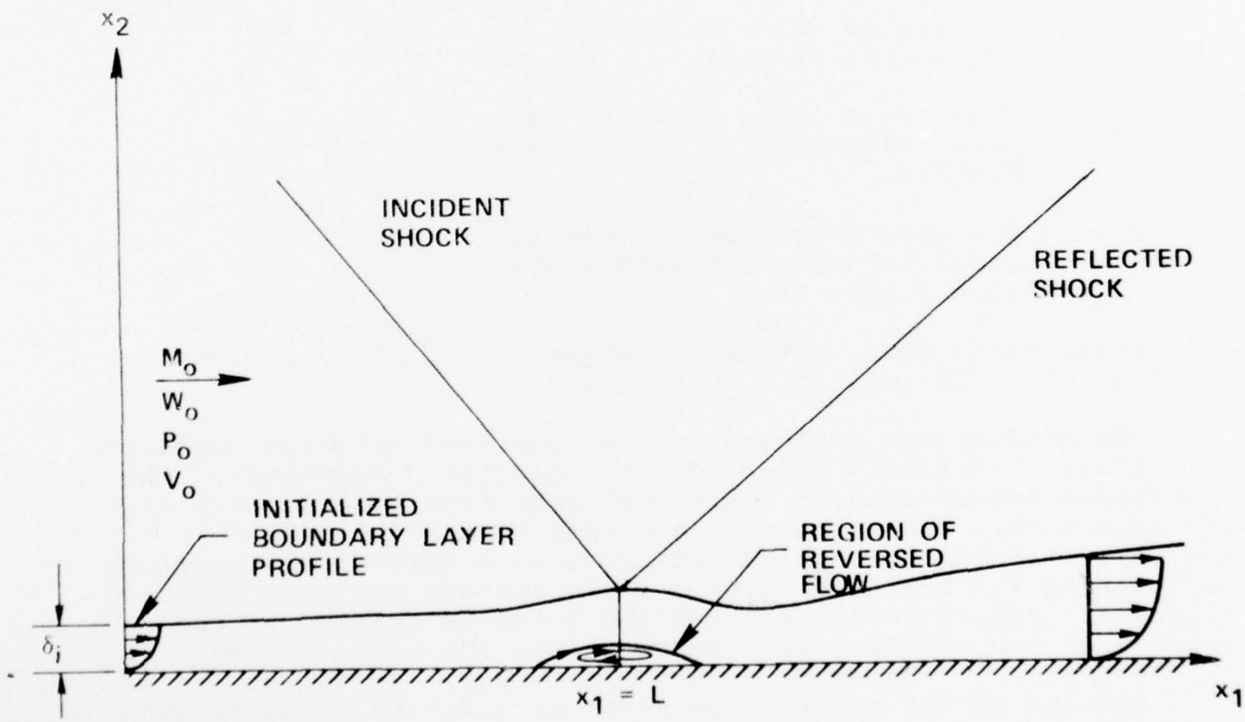

Figure 9. Generalized two-dimensional shock boundary layer interaction flow field.

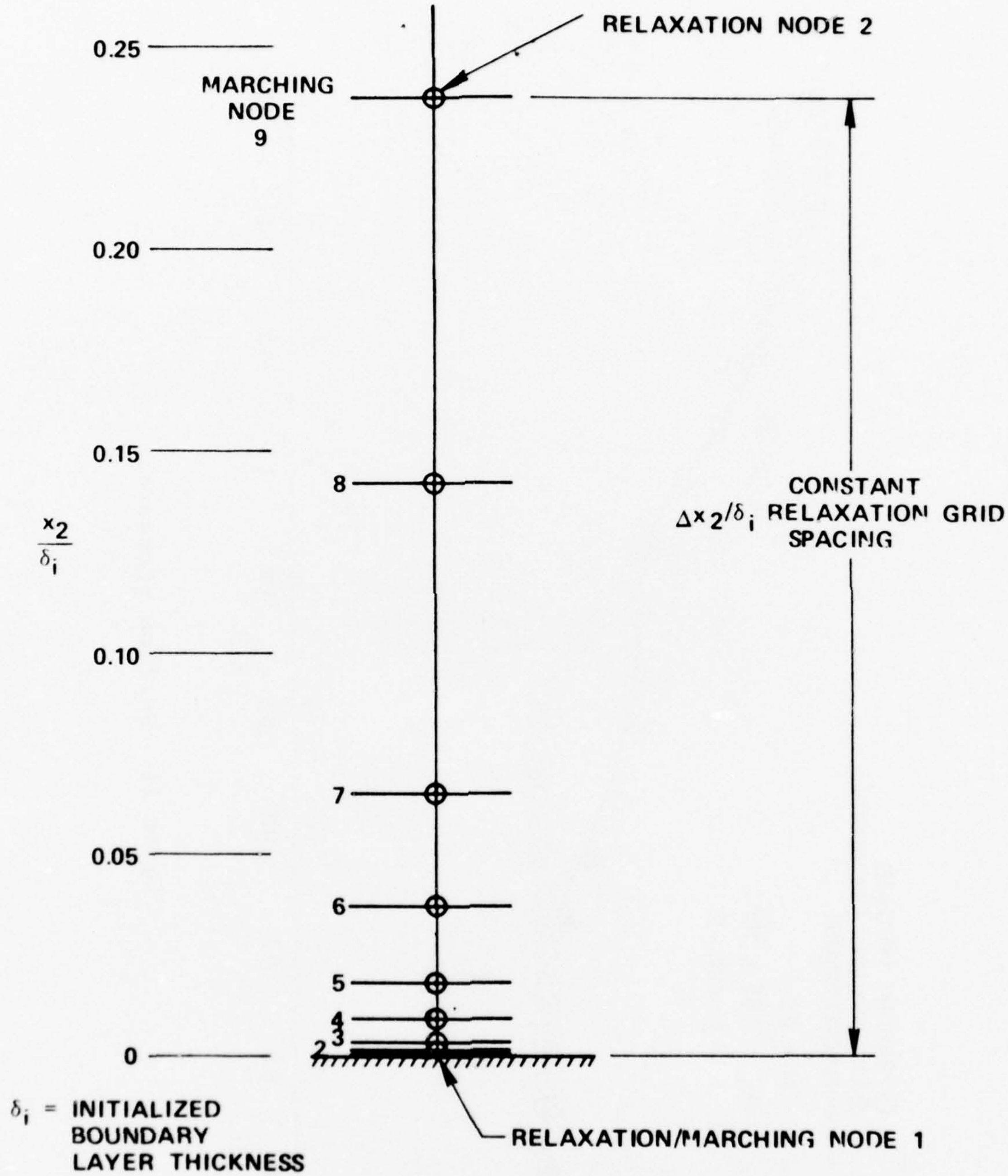

Figure 10. Relative relaxation and marching grid spacing.

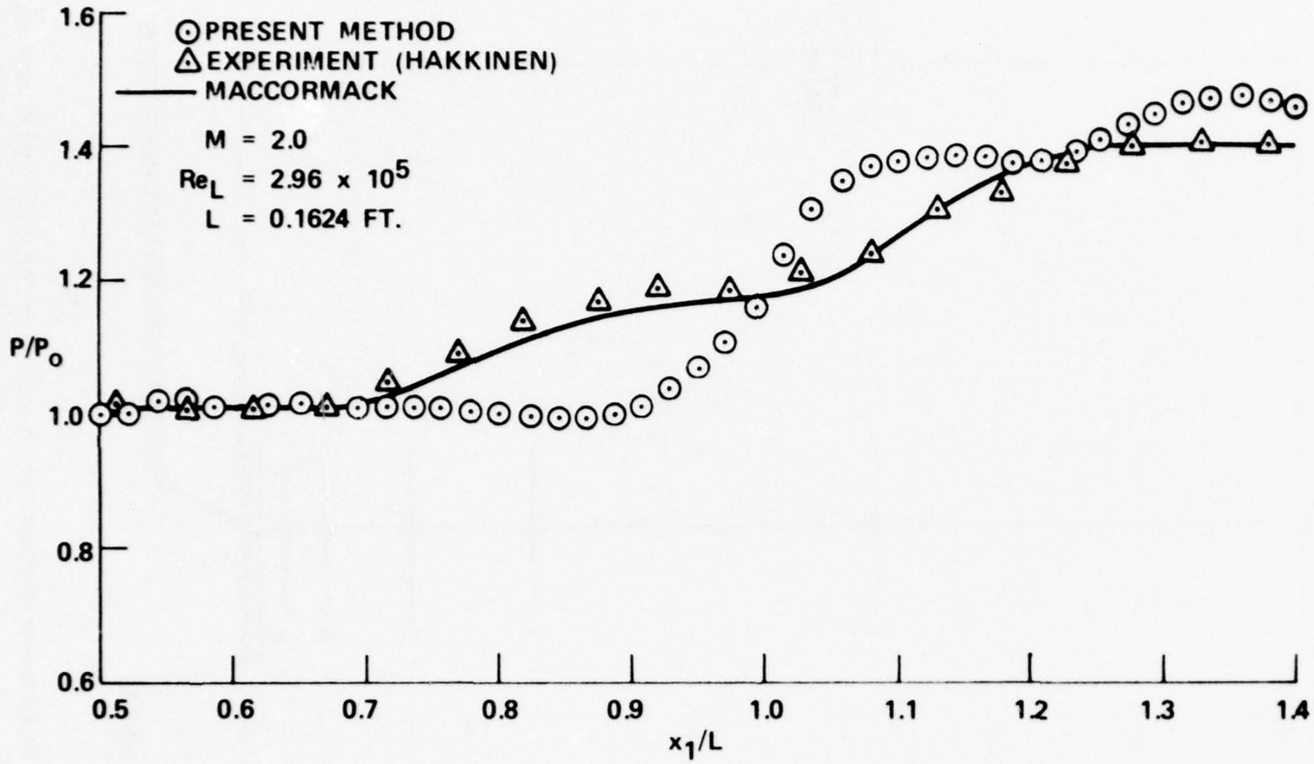

Figure 11. Surface pressure.

As a consequence of this too-sudden rise in static pressure, the predicted values of skin friction coefficient, C_f, shown in Figure 12, fail to decrease as far upstream as the experimental data. The predicted region of reversed flow is also much smaller than that indicated by Hakkinen's data.

The predicted values of C_f are presented as average values within a bandwidth of error representing the standard deviation of C_f as calculated at as many as 8 nodes within the constant pressure and density portion of the boundary layer. The skin friction coefficient is defined by

$$C_f = \frac{\rho_w \nu_w \frac{1}{h_2} \frac{\partial W_1}{\partial x_2}}{\frac{1}{2} \rho_\infty W_\infty{}^2}\Bigg|_w$$

where the subscript w refers to condition at the wall, and the subscript ∞ refers to the freestream. A considerable fluctuation in values of $\partial W_1/\partial x_2$ takes place, apparently due to the nonlinear character of the grid system near the plate.

Figures 13 through 15 are comparisons of boundary layer velocity profiles between the present steady-flow method and MacCormack's technique. In general, agreement is fair; however, once again it is apparent that the present method predicts a smaller region of separated flow, and generally larger displacement thicknesses. Discrepancies in the assumed inlet boundary layer profile are also apparent. Note that dimensions in the x_2 direction have been normalized by H_f (where $H_f = 0.003$ ft) -- a grid parameter used in MacCormack's data presentation.

Figure 16 presents static pressure contours over the solution space, based upon the results of the steady-flow method discussed here. The incident and reflected shocks are apparent, along with a spurious downstream reflection from the upper boundary of the region. The effect of the reflection is clearly visible in the downstream portion of the skin friction and surface pressure curves.

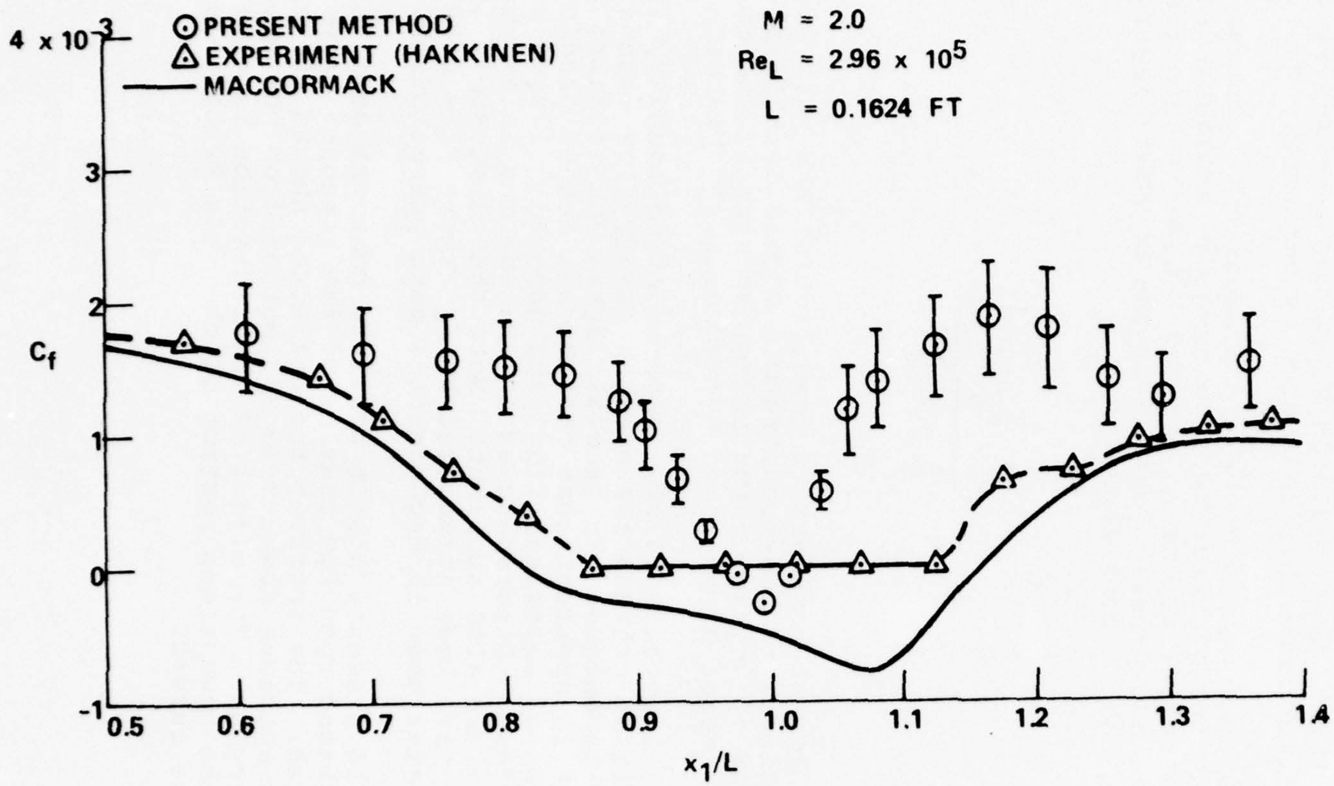

Figure 12. Skin friction coefficient.

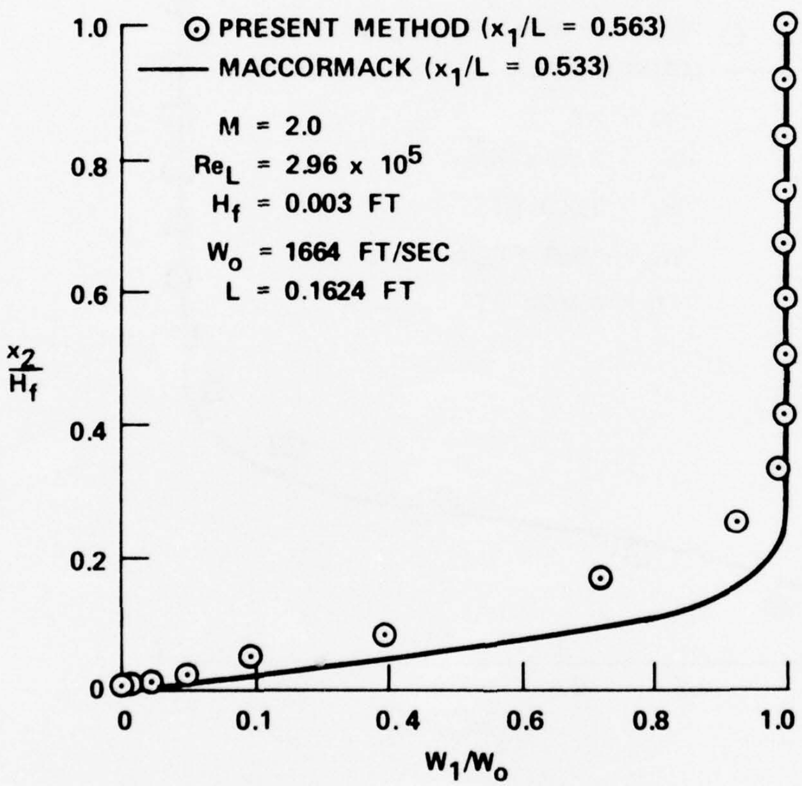

Figure 13. Velocity profile upstream of separation.

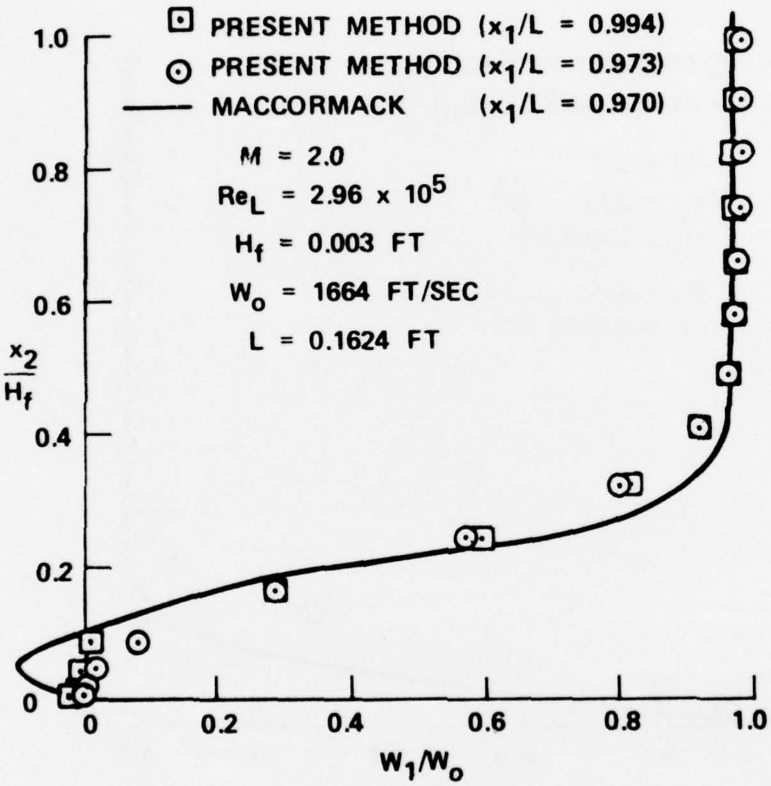

Figure 14. Velocity profile in region of shock wave.

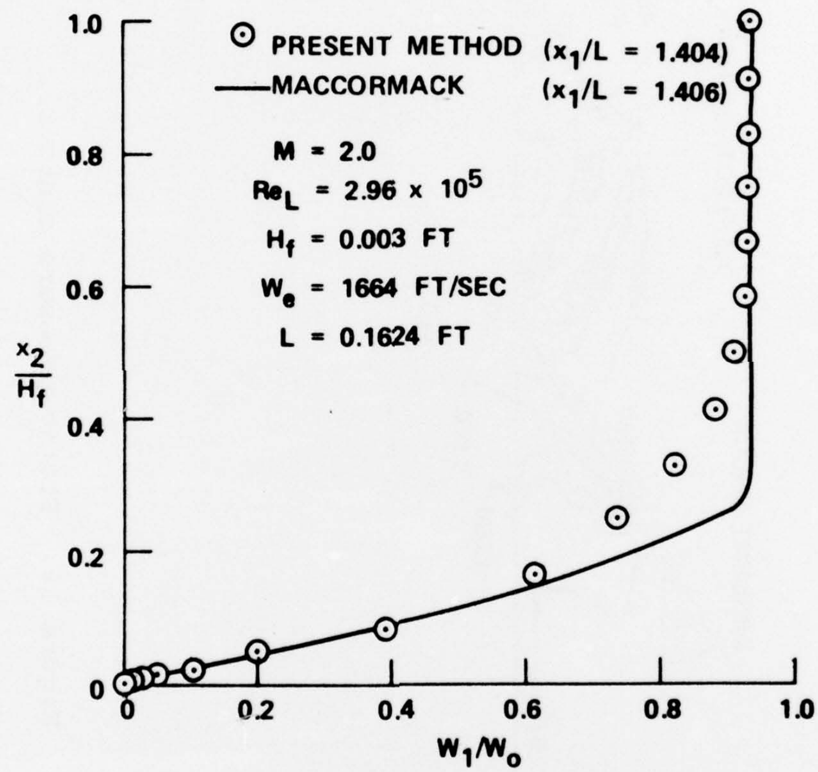

Figure 15. Velocity profile downstream of reattachment.

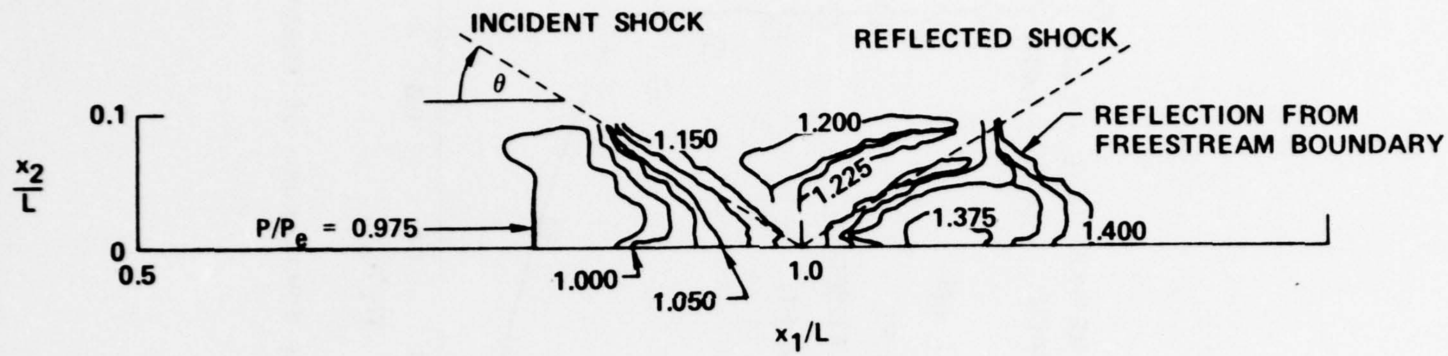

Figure 16. Static pressure contours.

SECTION V
HOW TO IMPROVE ACCURACY

Because of time and fiscal constraints, the development of this method halted with the results shown above. It is the opinion of the authors, based on an analysis of the computed results to date, that considerable improvements in accuracy are possible by improving the accuracy of both the relaxation and marching numerical methods. The relaxation nodes need only be a subset of the total grid. However, relaxation is responsible for satisfying the continuity equation. The effects of the increased displacement thickness downstream of the shock are propagated forward through the subsonic region of the flow field, creating the shock spreading observed above. It is of primary importance that this effect be properly accounted for. Figures 17 and 18 show the results of the above calculation on the mass balance of each grid element. In the relaxation grid, agreement is very good; but inside the marching-only region, substantial error occurs. This error comes about from several sources associated with the nonlinearity between the last relaxation node and the wall. A finite-difference approach to numerical method derivation assumes that a match of appropriate derivatives at a point yields a reasonable estimate of the founding equation in the vicinity of the match point. This is only true when variations in dependent variables are nearly linear, or at most quadratic. In a boundary layer, such as shown above, this assumption is in doubt. Substantial errors can occur in the numerical grid transformation, the evaluation of the source term for the relaxation equation, the evaluation of derivatives across the jump, and the like. The continuity error shown in Figures 17 and 18 is the result of the sum total of these effects. Undoubtly, a similar momentum and energy error also occur. The cure is to first produce a marching system that is derived from an integral equation. Thus, it can be integrally conservative through rapid changes in dependent variables. Secondly, an integral average for a source term of the potential equation must be established. As an example, for the position shown in Figure 17, $\nabla \cdot \vec{U}$, part of the source term, differs by a factor of 9 between the wall and the first relaxation node. The net effects of the source are not then well modeled by utilizing its value at the relaxation node, but rather a weighted average across the span would be needed. A grid system that is more nearly uniform would also help. It is obvious when examining the skin friction coefficient, as an example, that for W to deviate so far from linear very near the wall, there must be substantial error in the computation of the numerical transformation functions. The super position of two fixed-spaced grids, as utilized by MacCormack, would substantially alleviate this difficulty.

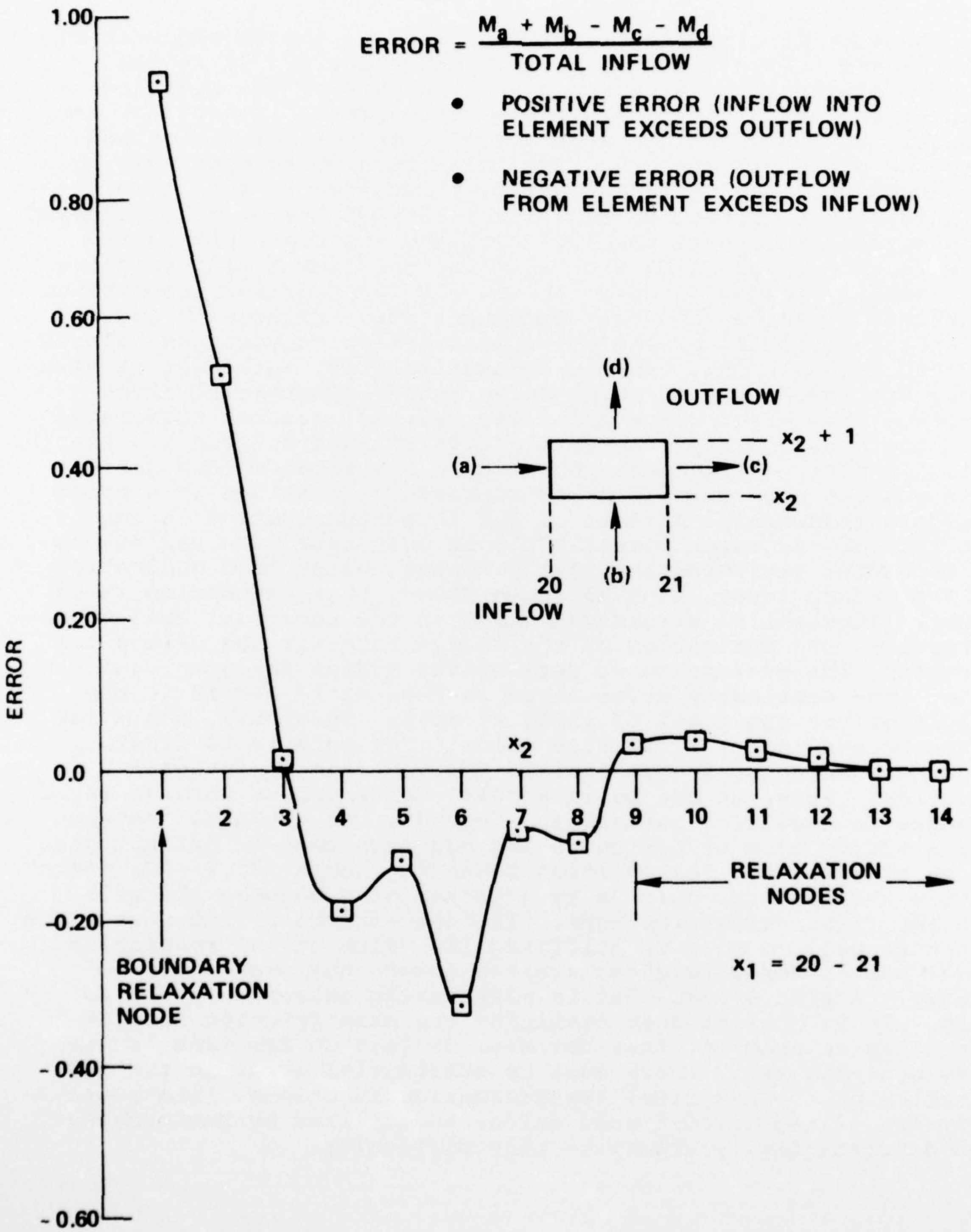

Figure 17. Element continuity error at x/L = 0.908.

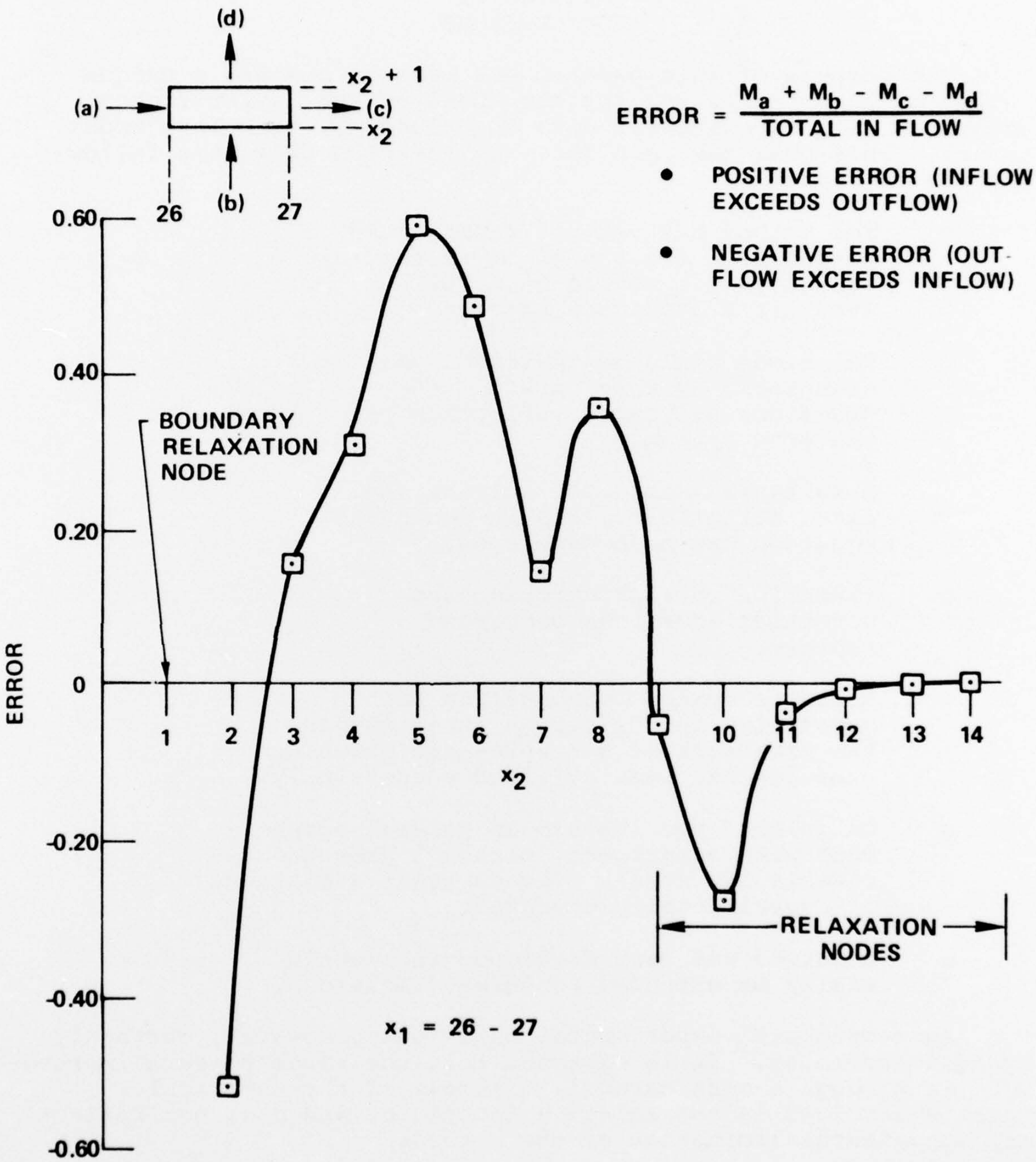

Figure 18. Element continuity error at x/L = 1.038.

SECTION VI
CONCLUSIONS

The purpose of this program has been to compare a unique method of numerically solving the steady-state Navier-Stokes equations with experimental data unconfused by turbulent model choice. This goal has been met. On the plus side, the following can be stated:

- The method has met its rapid speed potential, with run times in the vicinity of 1 minute on a CDC 7600 for a 3060 node problem.

  Run times could be improved substantially by more careful programming, and better selection of the grid system.

- A suitable method for solving the mixed elliptic-hyperbolic potential equation has been developed.

- Iteration between marching and potential equations converged rapidly.

- A simple method for handling both separation and diffusion terms within the framework of a single-pass marching equation has been utilized successfully.

- Calculated results are in general agreement with experiment, although pressure rise is not spread over as great a distance as experimentally observed.

- A method has been developed that could easily be extended to three-dimensions.

Agreement with experimental data could, however, certainly stand improvement. It is expected that the route to such improvement is through a more careful treatment of the numerical details involved in the solution technique, and does not reflect any fundamental limitation of the method.

SECTION VII
REFERENCES

1. Dodge, Paul R., "A Numerical Method for 2-D and 3-D Viscous Flows," AIAA Paper 76-425

2. Dodge, Paul R., and L.S. Lieber, "A Numerical Method for the Solution of the Navier-Stokes Equations with Separated Flow," AIAA Paper 77-170

3. Murman, E.M. and Cole, J.D., "Calculation of Plane Steady Transonic Flows," AIAA Journal, Vol. 9, No. 1, January 1971, pp 114-121

4. Dodge, Paul R., "A Nonorthogonal Numerical Method for Solving Transonic Cascade Flows," ASME 76-GT-63

5. Dodge, Paul R., "Transonic Two-Dimensional Flow Analysis of Compressor Cascade with Splitter Vanes," AFAPL-TR-75-110, September, 1975

6. Murman, E.M., "Analysis of Embedded Shock Waves Calculated by Relaxation Methods," Proceedings AIAA Computational Fluid Dynamics Conference, July 19-20, 1973

7. Hakkinen, R.J., Greber, I., Trilling, L., and Abarbauel, S.S., "The Interaction of an Oblique Shock Wave with a Laminar Boundary Layer," NASA Memo 2-18-59W, 1959

8. MacCormack, R.W., "An Efficient Numerical Method for Solving the Time-Dependent Compressible Navier-Stokes Equations at High Reynolds Number," NASA TM X-73, 124, July 1976

SECTION VIII
DISTRIBUTION

Technical Library
Building 313
Ballistic Research Laboratories
Aberdeen Proving Ground, MD 21005

Dr. F. D. Bennett
External Ballistic Laboratory
Ballistic Research Laboratories
Aberdeen Proving Ground, MD 21005

Mr. C. C. Hudson
Sandia Corporation
Sandia Base
Albuquerque, NM 81115

Professor P. J. Roache
Ecodynamics Research Associates, Inc.
P. O. Box 8172
Albuquerque, NM 87108

Dr. J. D. Shreve, Jr.
Sandia Corporation
Sandia Base
Albuquerque, NM 81115

Defense Documentation Center
Cameron Station, Building 5
Alexandria, VA 22314 12 Copies

Library
Naval Academy
Annapolis, MD 21402

Dr. G. H. Heilmeier
Director, Defense Advanced Research
Projects Agency
1400 Wilson Boulevard
Arlington, VA 22209

Mr. R. A. Moore
Deputy Director, Tactical Technology
Office
Defense Advanced Research Projects
Agency
1400 Wilson Boulevard
Arlington, VA 22209

Office of Naval Research
Code 411
Arlington, VA 22217

Office of Naval Research
Code 421
Arlington, VA 22217

Office of Naval Research
Code 438
Arlington, VA 22217

Office of Naval Research
Code 1021P (ONRL)
Arlington VA 22217 6 Copies

Dr. J. L. Potter
Deputy Director, Technology
von Karman Gas Dynamics Facility
Arnold Air Force Station, TN 37389

Professor J. C. Wu
Georgia Institute of Technology
School of Aerospace Engineering
Atlanta, GA 30332

Library
Aerojet-General Corporation
6352 North Irwindale Avenue
Azusa, CA 91702

NASA Scientific and Technical
Information Facility
P. O. Box 8757
Baltimore/Washington International
Airport, Maryland 21240

Dr. S. A. Berger
University of California
Department of Mechanical Engineering
Berkeley, CA 94720

Professor A. J. Chorin
University of California
Department of Mathematics
Berkeley, CA 94720

Professor M. Holt
University of California
Department of Mechanical Engineering
Berkeley, CA 94720

Dr. L. Talbot
University of California
Department of Mehcanical Engineering
Berkeley, CA 94720

Dr. H. R. Chaplin
Code 16
David W. Taylor Naval Ship Research and
Development Center
Bethesda, MD 20084

Code 1800
David W. Taylor Naval Ship Research and
Development Center
Bethesda, MD 20084

637-21

Code 5643
David W. Taylor Naval Ship Research and
Development Center
Bethesda, MD 20084

Dr. G. R. Inger
Virginia Polytechnic Institute and
State University
Department of Aerospace Engineering
Blacksburg, VA 24061

Professor A. H. Nayfeh
Virginia Polytechnic Institute and
State University
Department of Engineering Science and
Mechanics
Blacksburg, VA 24061

Indiana University
School of Applied Mathematics
Bloomington, IN 47401

Director
Office of Naval Research Branch Office
495 Summer Street
Boston, MA 02210

Supervisor, Technical Library Section
Thiokol Chemical Corporation
Wasatch Division
Brigham City, UT 84302

Dr. G. Hall
State University of New York at Buffalo
Faculty of Engineering and Applied
Science
Fluid and Thermal Sciences Laboratory
Buffalo, NY 14214

Mr. R. J. Vidal
Calspan Corporation
Aerodynamics Research Department
P. O. Box 235
Buffalo, NY 14221

Professor R. F. Probstein
Massachusetts Institute of Technology
Department of Mechanical Engineering
Cambridge, MS 02139

Director
Office of Naval Research Branch Office
536 South Clark Street
Chicago, IL 60605

Code 753
Naval Weapons Center
China Lake, CA 93555

Mr. J. Marshall
Code 4063
Naval Weapons Center
China Lake, CA 93555

637-22

Professor R. T. Davis
University of Cincinnati
Department of Aerospace Engineering and
Applied Mechanics
Cincinnati, OH 45221

Library MS 60-3
NASA Lewis Research Center
21000 Brookpark Road
Cleveland, OH 44135

Dr. J. D. Anderson, Jr.
Chairman, Department of Aerospace
Engineering
College of Engineering
University of Maryland
College Park, MD 20742

Professor W. L. Melnik
University of Maryland
Department of Aerospace Engineering
Glenn L. Martin Institute of Technology
College Park, MD 20742

Professor O. Burggraf
Ohio State University
Department of Aeronautical and
Astronautical Engineering
1314 Kinnear Road
Columbus, OH 43212

Technical Library
Naval Surface Weapons Center
Dahlgren Laboratory
Dahlgren, VA 22448

Dr. F. Moore
Naval Surface Weapons Center
Dahlgren Laboratory
Dahlgren, VA 22448

Technical Library 2-51131
LTV Aerospace Corporation
P. O. Box 5907
Dallas, TX 75222

Library, United Aircraft Corporation
Research Laboratories
Silver Lane
East Hartford, CT 06108

Technical Library
AVCO-Everett Research Laboratory
2385 Revere Beach Parkway
Everett, MA 02149

Professor G. Moretti
Polytechnic Institute of New York
Long Island Center
Department of Aerospace Engineering
and Applied Mechanics
Route 110
Farmingdale, NY 11735

Professor S. G. Rubin
Polytechnic Institute of New York
Long Island Center
Department of Aerospace Engineering
and Applied Mechanics
Route 110
Farmingdale, NY 11735

Technical Documents Center
Army Mobility Equipment R&D Center
Building 315
Fort Belvoir, VA 22060

Dr. W. R. Briley
Scientific Research Associates, Inc.
P.O. Box 498
Glastonbury, CT 06033

Library (MS 185)
NASA Langley Research Center
Langley Station
Hampton, VA 23665

Dr. S. Nadir
Northrop Corporation
Aircraft Division
3901 West Broadway
Hawthorne, CA 90250

Professor A. Chapmann
Chairman, Mechanical Engineering
Department
William M. Rice Institute
Box 1892
Houston, TX 77001

Dr. F. Lane
KLD Associates, Inc.
7 High Street
Huntington, NY 11743

Technical Library
Naval Ordnance Station
Indian Head, MD 20640

Professor D. A. Caughey
Cornell University
Sibley School of Mechanical and
Aerospace Engineering
Ithaca, NY 14853

Professor E. L. Resler
Cornell University
Sibley School of Mechanical and
Aerospace Engineering
Ithaca, NY 14853

Professor S. F. Shen
Cornell University
Sibley School of Mechanical and
Aerospace Engineering
Ithaca, NY 14853

Library
Midwest Research Institute
425 Volker Boulevard
Kansas City, MO 64110

Dr. M. M. Hafez
Flow Research, Inc.
P. O. Box 5040
Kent, WA 98031

Dr. E. M. Murman
Flow Research, Inc.
P.O. Box 5040
Kent, WA 98031

Dr. S. A. Orszag
Cambridge Hydrodynamics, Inc.
54 Baskin Road
Lexington, MA 02173

Professor T. Cebeci
California State University. Long Beach
Mechanical Engineering Department
Long Beach, CA 90840

Mr. J. L. Hess
Douglas Aircraft Company
3855 Lakewood Boulevard
Long Beach, CA 90808

Dr. H. K. Cheng
University of Southern California,
University Park
Department of Aerospace Engineering
Los Angeles, CA 90007

Professor J. D. Cole
University of California
Mechanics and Structures Department
School of Engineering and Applied
Science
Los Angeles, CA 90024

Engineering Library
University of Southern California
Box 77929
Los Angeles, CA 90007

Dr. C. M. Ho
University of Southern California,
University Park
Department of Aerospace Engineering
Los Angeles, CA 90007

Dr. T. D. Taylor
The Aerospace Corporation
P. O. Box 92957
Los Angeles, CA 90009

Commanding Officer
Naval Ordance Station
Louisville, KY 40214

637-25

Mr. B. H. Little, Jr.
Lockheed-Georgia Company
Department 72-74, Zone 369
Marietta, GA 30061

Dr. C. Cook
Stanford Research Institute
Menlo Park, CA 94025

Professor E. R. G. Eckert
University of Minnesota
241 Mechanical Engineering Building
Minneapolis, MN 55455

Library
Naval Postgraduate School
Monterey, CA 93940

McGill University
Supersonic-Gas Dynamics Research
Laboratory
Department of Mechanical Engineering
Montreal 12, Quebec, Canada

Librarian
Engineering Library, 127-223
Radio Corporation of America
Morristown, NJ 07960

Dr. S. S. Stahara
Nielsen Engineering & Research, Inc.
510 Clyde Avenue
Mountain View, CA 94043

Engineering Societies Library
345 East 47th Street
New York, NY 10017

Professor A. Jameson
New York University
Courant Institute of Mathematical
Sciences
251 Mercer Street
New York, NY 10012

Professor G. Miller
New York University
Department of Applied Science
26-36 Stuyvesant Street
New York, NY 10003

Office of Naval Research
New York Area Office
715 Broadway - 5th Floor
New York, NY 10003

Dr. A. Vaglio-Laurin
New York University
Department of Applied Science
26-36 Stuyvesant Street
New York, NY 10003

637-26

Professor S. Weinbaum
Research Foundation of the City
University of New York on behalf
of the City College
1411 Broadway
New York, NY 10018

Librarian, Aeronautical Library
National Research Council
Montreal Road
Ottawa 7, Canada

Lockheed Missiles and Space Company
Technical Information Center
3251 Hanover Street
Palo Alto, CA 94304

Director
Office of Naval Research Branch Office
1030 East Green Street
Pasadena, CA 91106

California Institute of Technology
Engineering Division
Pasadena, CA 91109

Library
Jet Propulsion Laboratory
4800 Oak Grove Drive
Pasadena, CA 91103

Professor H. Liepmann
California Institute of Technology
Department of Aeronautics
Pasadena, CA 91109

M. L. I. Chasen, MGR-MSD Library
General Electric Company
Missile and Space Division
P. O. Box 8555
Philadelphia, PA 19101

Mr. P. Dodge
AiResearch Manufacturing Company
Division of Garrett Corporation
402 South 36th Street
Phoenix, AZ 85034

Technical Library
Naval Missile Center
Point Mugu, CA 93042

Professor S. Bogdonoff
Princeton University
Gas Dynamics Laborary
Department of Aerospace and
Mechanical Sciences
Princeton, NJ 08540

637-27

Professor S. I. Cheng
Princeton University
Department of Aerospace and
Mechanical Sciences
Princeton, NJ 08540

Dr. J. E. Yates
Aeronautical Research Associates
of Princeton, Inc.
50 Washington Road
Princeton, NJ 08540

Professor J. H. Clarke
Brown University
Division of Engineering
Providence, RI 02912

Professor J. T. C. Liu
Brown University
Division of Engineering
Providence, RI 02912

Professor L. Sirovich
Brown University
Division of Applied Mathematics
Providence, RI 02912

Dr. P. K. Dai (R1/2178)
TRW Systems Group, Inc.
One Space Park
Redondo Beach, CA 90278

Redstone Scientific Information
Center
Chief, Document Section
Army Missile Command
Redstone Arsenal, AL 35809

U.S. Army Research Office
P. O. Box 12211
Research Triangle, NC 27709

Professor M. Lessen
The University of Rochester
Department of Mechanical Engineering
River Campus Station
Rochester, NY 14627

Editor, Applied Mechanics Review
Southwest Research Institute
8500 Culebra Road
San Antonio, TX 78228

Library and Information Services
General Dynamics-CONVAIR
P. O. Box 1128
San Diego, CA 92112

Dr. R. Magnus
General Dynamics-CONVAIR
Kearny Mesa Plant
P. O. Box 80847
San Diego, CA 92138

637-28

Mr. T. Brundage
Defense Advanced Research
Projects Agency
Research and Development
Field Unit
APO 146, Box 271
San Francisco, CA 96246

Office of Naval Research
San Francisco Area Office
760 Market Street - Room 447
San Francisco, CA 94102

Library
The Rand Corporation
1700 Main Street
Santa Monica, CA 90401

Department Librarian
University of Washington
Department of Aeronautics and
Astronautics
Seattle, WA 98105

Dr. P. E. Rubbert
Boeing Commercial Airplane Company
P.O. Box 3707
Seattle, WA 98124

Mr. R. Feldhuhn
Naval Surface Weapons Center
White Oak Laboratory
Silver Spring, MD 20910

Dr. G. Heiche
Naval Surface Weapons Center
Mathematical Analysis Branch
Silver Spring, MD 20910

Librarian
Naval Surface Weapons Center
White Oak Laboratory
Silver Spring, MD 20910

Dr. J. M. Solomon
Naval Surface Weapons Center
White Oak Laboratory
Silver Spring, MD 20910

Professor J. H. Ferziger
Stanford University
Department of Mechanical Engineering
Stanford, CA 94305

Professor K. Karamchetic
Stanford University
Department of Aeronautics and
Astronautics
Stanford, CA 94305

371-24

Professor M. van Dyke
Stanford University
Department of Aeronautics and
Astronautics
Stanford, CA 94305

Engineering Library
McDonnell Douglas Corporation
Department 218, Building 101
P. O. Box 516
St. Louis, MO 63166

Dr. R. J. Hakkinen
McDonnell Douglas Corporation
Department 222
P. O. Box 516
St. Louis, MO 63166

Dr. R. P. Heinisch
Honeywell, Inc.
Systems and Research Division -
Aerospace Defense Group
2345 Walnut Street
St. Paul, MN 55113

Professor R. G. Stoner
Arizona State University
Department of Physics
Tempe, AZ 85281

Dr. N. Malmuth
Rockwell International
Science Center
1049 Camino Dos Rios
P. O. Box 1085
Thousand Oaks, CA 91360

Rockwell International
Science Center
1049 Camino Dos Rios
P. O. Box 1085
Thousand Oaks, CA 91360

The Library
University of Toronto
Institute of Aerospace Studies
Toronto 5, Canada

Professor W. R. Sears
University of Arizona
Aerospace and Mechanical Engineering
Tucson, AZ 85721

Professor A. R. Seebass
University of Arizona
Department of Aerospace and
Mechanical Engineering
Tucson, AZ 85721

Dr. S. M. Yen
University of Illinois
Coordinated Science Laboratory
Urbana, IL 61801

371-25

Dr. K. T. Yen
Code 3015
Naval Air Development Center
Warminster, PA 18974

Air Force Office of Scientific
Research (SREM)
Building 1410, Bolling AFB
Washington, DC 20332

Chief of Research & Development
Office of Chief of Staff
Department of the Army
Washington, DC 20310

Library of Congress
Science and Technology Division
Washington, DC 20540

Director of Research (Code RR)
National Aeronautics and
Space Administration
600 Independence Avenue, SW
Washington, DC 20546

Library
National Bureau of Standards
Washington, DC 20234

National Science Foundation
Engineering Division
1800 G Street, NW
Washington, DC 20550

Mr. W. Koven (AIR 03E)
Naval Air Systems Command
Washington, DC 20361

Mr. R. Siewert (AIR 320D)
Naval Air Systems Command
Washington, DC 20361

Technical Library Division (AIR 604)
Naval Air Systems Command
Washington, DC 20361

Code 2627
Naval Research Laboratory
Washington, DC 20375

SEA 03512
Naval Sea Systems Command
Washington, DC 20362

SEA 09G3
Naval Sea Systems Command
Washington, DC 20362

Dr. A. L. Slafkosky
Scientific Adviser
Commandant of the Marine Corps
(Code AX)
Washington, DC 20380

Director
Weapons Systems Evaluation Group
Washington, DC 20305

Dr. P. Baronti
General Applied Science
Laboratories, Inc.
Merrick and Stewart Avenues
Westbury, NY 11590

Bell Laboratories
Whippany Road
Whippany, NJ 07981

Chief of Aerodynamics
AVCO Corporation
Missile Systems Division
201 Lowell Street
Wilmington, MA 01887

Research Library
AVCO Cororation
Missile Systems Division
201 Lowell Street
Wilmington, MA 01887

AFAPL (APRC)
AB
Wright Patterson AFB, OH 45433

Dr. Donald J. Harney
AFFDL/FX
Wright Patterson AFB, OH 45433